

Analysis of thick isotropic and cross-ply laminated plates by Generalized Differential Quadrature Method and a Unified Formulation.

*Original*

Analysis of thick isotropic and cross-ply laminated plates by Generalized Differential Quadrature Method and a Unified Formulation / Tornabene, F.; Fantuzzi, N.; Viola, E.; Cinefra, Maria; Carrera, Erasmo; Ferreira, A. J. M.; Zenkour, A. M.. - In: COMPOSITES. PART B, ENGINEERING. - ISSN 1359-8368. - 58:(2014), pp. 544-552. [10.1016/j.compositesb.2013.10.088]

*Availability:*

This version is available at: 11583/2517097 since:

*Publisher:*

Elsevier

*Published*

DOI:10.1016/j.compositesb.2013.10.088

*Terms of use:*

This article is made available under terms and conditions as specified in the corresponding bibliographic description in the repository

*Publisher copyright*

(Article begins on next page)

# Analysis of Thick Isotropic and Cross-Ply Laminated Plates by Generalized Differential Quadrature Method and a Unified Formulation

F. Tornabene<sup>c</sup>, N. Fantuzzi<sup>c</sup>, E. Viola<sup>c</sup>, M. Cinefra<sup>b</sup>, E. Carrera<sup>b,d</sup>, A.J.M. Ferreira<sup>a,d</sup>, A. M. Zenkour<sup>d,e</sup>

<sup>a</sup>*Faculdade de Engenharia da Universidade do Porto, Porto, Portugal*

<sup>b</sup>*Department of Aeronautics and Aerospace Engineering, Politecnico di Torino, Corso Duca degli Abruzzi, 24, 10129 Torino, Italy*

<sup>c</sup>*DICAM Department, Alma Mater Studiorum University of Bologna, Viale del Risorgimento, 2, 40136 Bologna, Italy*

<sup>d</sup>*Department of Mathematics, Faculty of Science, King Abdulaziz University, P.O. Box 80203, Jeddah 21589, Saudi Arabia*

<sup>e</sup>*Department of Mathematics, Faculty of Science, Kafrelsheikh University, Kafr El-Sheikh 33516, Egypt*

---

## Abstract

In this paper, the Carrera Unified Formulation and the generalized differential quadrature technique are combined for predicting the static deformations and the free vibration behavior of thin and thick isotropic as well as cross-ply laminated plates. Through numerical experiments, the capability and efficiency of this technique, based on the strong formulation of the problem equations, are demonstrated. The numerical accuracy and convergence are also examined. It is worth noting that all the presented numerical examples are compared with both literature and numerical solutions obtained with a finite element code. The proposed methodology appears to be able to deal not only with uniform boundary conditions, such as fully clamped or completely simply-supported, but also with mixed external conditions, that can be clamped, supported or free.

---

## Keywords

A.Laminates; B.Vibration; C.Computational Modelling

## 1. Introduction

In this paper the Unified Formulation (UF) proposed by Carrera [1–5] is used to derive the equations of motion and boundary conditions and to analyse isotropic and cross-ply laminated plates by the generalized differential quadrature (GDQ) method. A higher order theory (HSDT) as proposed before by Kant [6, 7] considering non-zero normal deformation  $\varepsilon_z$  is adopted, and an expanded higher-order shear deformation up to the cubic expansion in  $z$  for all in-plane displacement components is worked out.

The combination of the UF and collocation with the GDQ method provides an easy, highly accurate framework for the solution to plates, under any kind of shear deformation theory, irrespective of the geometry, loads or boundary conditions. In this sense, this methodology can be considered a generalized UF.

Many shear deformation theories, that involve a constant transverse displacement across the thickness direction and make the transverse normal strain and stress negligible, were proposed. This assumption is adequate for thin-plates or plates for which the thickness-to-side  $h/a$  is smaller than 0.1. For higher  $h/a$  ratios, the use of shear deformation theories including the contribution of the transverse normal strain and stress is fundamental. Among such theories, the pioneering higher-order plate theory by Lo et al. [8, 9] or the ones by Kant and colleagues [6, 7] can be cited. Recently, the works by Batra [10] and Carrera [1, 2, 11] show interesting ways of computing transverse and normal stresses in laminated composite or sandwich plates. Higher-order theories in the thickness direction were also addressed by Librescu et al. [12], Reddy [13] and more recently by Fiedler and colleagues [14], who considered polynomial expansions in the thickness direction. None of such approaches carried out the analysis by the GDQ method. Some other HSDTs have been presented over the years regarding composite materials, FGMs as well as beams, plates and shells [15–19], however it is impossible to cite them all. The use of alternative methods, such as meshless methods based on generalized differential quadrature, is attractive due to the absence of a mesh and

the use of strong-form methods. The present work adds some numerical applications and results to the vast bibliography concerning meshless methods [20–45].

In this paper, it is investigated for the first time how the UF by Carrera can be combined with the GDQ method for treating thick isotropic and cross-ply laminated plates, using a refined higher-order shear and normal deformation theory. The quality of the present method in predicting static deformations, and free vibrations of thick isotropic and cross-ply laminated plates is compared and discussed with other methods in some numerical examples.

## 2. Fundamental equations via Unified Formulation

Many details of the Unified Formulation (UF) by Carrera can be inspected in [1–4, 11]. In the present section the equations of motion and the corresponding boundary conditions are worked out by using the fundamental nuclei [1–4, 11] and a compact matrix form notation.

### 2.1. Displacement field

By defining a displacement field, that involves all layers, an equivalent single-layer theory is proposed. The displacement field is expressed as

$$\begin{aligned} U &= u_0 + zu_1 + z^3u_2 \\ V &= v_0 + zv_1 + z^3v_2 \\ W &= w_0 + zw_1 + z^2w_2 \end{aligned} \tag{1}$$

The kinematic hypothesis (1) can be generally written, using the UF, as

$$\begin{aligned} U &= F_0u^{(0)} + F_1u^{(1)} + F_2u^{(2)} \\ V &= F_0v^{(0)} + F_1v^{(1)} + F_2v^{(2)} \\ W &= F_0w^{(0)} + F_1w^{(1)} + F_2w^{(2)} \end{aligned} \tag{2}$$

where  $F_\tau$ , for  $\tau = 0, 1, 2$ , are the thickness functions. In particular, for the in-plane displacements  $(F_0, F_1, F_2) = (1, z, z^3)$  and for the out-of-plane displacement  $(F_0, F_1, F_2) = (1, z, z^2)$ . In conclusion, the displacement field (2) can be written in compact matrix form using the

following recursive formula

$$\mathbf{U} = \sum_{\tau=0}^2 \mathbf{F}_{\tau} \mathbf{u}^{(\tau)} \quad (3)$$

where  $\mathbf{U} = [U(x, y, z, t) \ V(x, y, z, t) \ W(x, y, z, t)]^T$  is the three dimensional displacement vector and  $\mathbf{u}^{(\tau)} = [u^{(\tau)}(x, y, t) \ v^{(\tau)}(x, y, t) \ w^{(\tau)}(x, y, t)]^T$  is the  $\tau$ th order generalized displacement component vector of the middle surface points ( $z = 0$ ).  $\mathbf{F}_{\tau}$  is a  $3 \times 3$  matrix, that is

$$\mathbf{F}_{\tau} = \begin{bmatrix} F_{\tau} & 0 & 0 \\ 0 & F_{\tau} & 0 \\ 0 & 0 & F_{\tau} \end{bmatrix} \quad (4)$$

This corresponds to a refined, higher-order shear deformation theory, as initially proposed by Kant [6]. For a laminate with  $n$  orthotropic layers, the lower and upper layer surfaces are defined by  $z_k$  and  $z_{k+1}$ , respectively, as illustrated in figure 1 for a 3-layered laminate. Since a laminated plate is taken into account, it should be also mentioned that the total plate thickness  $h$  is given by the following sum

$$h = \sum_{k=1}^l h_k \quad (5)$$

where  $h_k = z_{k+1} - z_k$  is the generic thickness of the  $k$ th lamina and  $l$  is the total number of layers.

## 2.2. Deformation components

The generalized strain component vector of the  $\tau$ th order following the UF approach can be written as

$$\boldsymbol{\varepsilon}^{(\tau)} = \mathbf{D}_{\Omega} \mathbf{u}^{(\tau)}, \text{ for } \tau = 0, 1, 2 \quad (6)$$

where  $\boldsymbol{\varepsilon}^{(\tau)} = [\varepsilon_x^{(\tau)} \ \varepsilon_y^{(\tau)} \ \gamma_x^{(\tau)} \ \gamma_y^{(\tau)} \ \gamma_{xz}^{(\tau)} \ \gamma_{yz}^{(\tau)} \ \omega_{xz}^{(\tau)} \ \omega_{yz}^{(\tau)} \ \varepsilon_z^{(\tau)}]^T$  and  $\mathbf{D}_{\Omega}$  is the kinematic partial differential operator

$$\mathbf{D}_{\Omega} = \begin{bmatrix} \frac{\partial}{\partial x} & 0 & 0 & \frac{\partial}{\partial y} & 0 & 0 & 1 & 0 & 0 \\ 0 & \frac{\partial}{\partial y} & \frac{\partial}{\partial x} & 0 & 0 & 0 & 0 & 1 & 0 \\ 0 & 0 & 0 & 0 & \frac{\partial}{\partial x} & \frac{\partial}{\partial y} & 0 & 0 & 1 \end{bmatrix}^T \quad (7)$$

### 2.3. Stress components

The constituent material of the given plate layers is linearly elastic, thus, the constitutive equations in terms of stresses are defined lamina per lamina. The stress components are given by the Hooke law [13]

$$\boldsymbol{\sigma}^{(k)} = \bar{\mathbf{C}}^{(k)} \boldsymbol{\varepsilon}^{(k)} \quad (8)$$

where the stress component vector means  $\boldsymbol{\sigma}^{(k)} = [\sigma_x^{(k)} \ \sigma_y^{(k)} \ \tau_{xy}^{(k)} \ \tau_{xz}^{(k)} \ \tau_{yz}^{(k)} \ \sigma_z^{(k)}]^T$ , the strain component vector is indicated as  $\boldsymbol{\varepsilon}^{(k)} = [\varepsilon_x^{(k)} \ \varepsilon_y^{(k)} \ \gamma_{xy}^{(k)} \ \gamma_{xz}^{(k)} \ \gamma_{yz}^{(k)} \ \varepsilon_z^{(k)}]^T$  and  $\bar{\mathbf{C}}^{(k)}$  is the constitutive matrix for the  $k$ th lamina. For the sake of completeness the matrix at hand is reported below

$$\bar{\mathbf{C}}^{(k)} = \begin{bmatrix} \bar{C}_{11}^{(k)} & \bar{C}_{12}^{(k)} & \bar{C}_{16}^{(k)} & 0 & 0 & \bar{C}_{13}^{(k)} \\ \bar{C}_{12}^{(k)} & \bar{C}_{22}^{(k)} & \bar{C}_{26}^{(k)} & 0 & 0 & \bar{C}_{23}^{(k)} \\ \bar{C}_{16}^{(k)} & \bar{C}_{26}^{(k)} & \bar{C}_{66}^{(k)} & 0 & 0 & \bar{C}_{36}^{(k)} \\ 0 & 0 & 0 & \bar{C}_{44}^{(k)} & \bar{C}_{45}^{(k)} & 0 \\ 0 & 0 & 0 & \bar{C}_{45}^{(k)} & \bar{C}_{55}^{(k)} & 0 \\ \bar{C}_{13}^{(k)} & \bar{C}_{23}^{(k)} & \bar{C}_{36}^{(k)} & 0 & 0 & \bar{C}_{33}^{(k)} \end{bmatrix} \quad (9)$$

In equation (9)  $\bar{C}_{nm}^{(k)}$ , for  $n, m = 1, 2, \dots, 6$ , represent the material constants in the Cartesian reference system, after the equations of transformation [13] are applied. By integrating the stress components through the thickness of the plate, the stress resultants are obtained

$$\mathbf{S}^{(\tau)} = \sum_{s=0}^2 \mathbf{A}^{(\tau s)} \boldsymbol{\varepsilon}^{(s)}, \text{ for } \tau = 0, 1, 2 \quad (10)$$

where  $\mathbf{S}^{(\tau)} = [N_x^{(\tau)} \ N_y^{(\tau)} \ N_{xy}^{(\tau)} \ N_{yx}^{(\tau)} \ T_x^{(\tau)} \ T_y^{(\tau)} \ P_x^{(\tau)} \ P_y^{(\tau)} \ S_z^{(\tau)}]^T$  and  $\mathbf{A}^{(\tau s)}$  are the stiffness constants [39] that can be evaluated as

$$\begin{aligned} A_{nm}^{(\tau s)} &= \sum_{k=1}^l \int_{z_k}^{z_{k+1}} \bar{C}_{nm}^{(k)} F_s F_\tau dz \\ A_{nm}^{(\bar{\tau} s)} &= \sum_{k=1}^l \int_{z_k}^{z_{k+1}} \bar{C}_{nm}^{(k)} F_s \frac{\partial F_\tau}{\partial z} dz \quad \text{for } \tau, s = 0, 1, 2 \\ A_{nm}^{(\tau \bar{s})} &= \sum_{k=1}^l \int_{z_k}^{z_{k+1}} \bar{C}_{nm}^{(k)} \frac{\partial F_s}{\partial z} F_\tau dz \quad \text{for } n, m = 1, 2, \dots, 6 \\ A_{nm}^{(\bar{\tau} \bar{s})} &= \sum_{k=1}^l \int_{z_k}^{z_{k+1}} \bar{C}_{nm}^{(k)} \frac{\partial F_s}{\partial z} \frac{\partial F_\tau}{\partial z} dz \end{aligned} \quad (11)$$

In equation (11) the indices  $\tau, s$  are related to the chosen thickness functions  $F_\tau, F_s$ . When these indices are indicated as  $\tilde{\tau}, \tilde{s}$ , it means that the corresponding thickness functions are derived with respect to  $z$ , that is  $\partial F_\tau / \partial z, \partial F_s / \partial z$ . The subscripts  $n, m$  of equation (11) follow the relationships shown in equation (11) itself.

#### 2.4. Equations of motion

The static equilibrium equations can be deduced from the principle of virtual displacements [39] as

$$\mathbf{D}_\Omega^* \mathbf{S}^{(\tau)} + \mathbf{q}^{(\tau)} = \sum_{s=0}^2 \mathbf{M}^{(\tau s)} \ddot{\mathbf{u}}^{(s)}, \text{ for } \tau = 0, 1, 2 \quad (12)$$

where  $\mathbf{q}^{(\tau)}$  is the static load vector of the forces applied upon the shell middle surface. It should be noted that the vector at hand is defined as

$$\begin{aligned} q_x^{(\tau)} &= q_x^{(-)} F_\tau^{(-)} + q_x^{(+)} F_\tau^{(+)} \\ q_y^{(\tau)} &= q_y^{(-)} F_\tau^{(-)} + q_y^{(+)} F_\tau^{(+)} \\ q_z^{(\tau)} &= q_z^{(-)} F_\tau^{(-)} + q_z^{(+)} F_\tau^{(+)} \end{aligned} \quad (13)$$

where  $q_x^{(-)}, q_y^{(-)}, q_z^{(-)}$  and  $q_x^{(+)}, q_y^{(+)}, q_z^{(+)}$  are the forces applied at the bottom  $(-)$  and top  $(+)$  surfaces of the plate, respectively. On the other hand,  $\mathbf{D}_\Omega^*$  is the equilibrium operator, that can be written in matrix form [39] as

$$\mathbf{D}_\Omega^* = \begin{bmatrix} \frac{\partial}{\partial x} & 0 & 0 & \frac{\partial}{\partial y} & 0 & 0 & -1 & 0 & 0 \\ 0 & \frac{\partial}{\partial y} & \frac{\partial}{\partial x} & 0 & 0 & 0 & 0 & -1 & 0 \\ 0 & 0 & 0 & 0 & \frac{\partial}{\partial x} & \frac{\partial}{\partial y} & 0 & 0 & -1 \end{bmatrix} \quad (14)$$

The inertia matrix  $\mathbf{M}^{(\tau s)}$  has the form

$$\mathbf{M}^{(\tau s)} = \begin{bmatrix} I_0^{(\tau s)} & 0 & 0 \\ 0 & I_0^{(\tau s)} & 0 \\ 0 & 0 & I_0^{(\tau s)} \end{bmatrix} \text{ for } \tau, s = 0, 1, 2 \quad (15)$$

in which the mass inertia terms  $I_0^{(\tau s)}$  are defined by

$$I_0^{(\tau s)} = \sum_{k=1}^l \int_{z_k}^{z_{k+1}} \rho^{(k)} F_\tau F_s dz, \text{ for } \tau, s = 0, 1, 2 \quad (16)$$

In expression (16)  $\rho^{(k)}$  is the mass density per unit of volume of the  $k$ th ply. In order to carry out the equation of motion in terms of displacement components the kinematic (6), constitutive (10) and equilibrium (12) equations have to be combined. The resultant partial differential system of equations can be written in compact matrix form as

$$\sum_{s=0}^2 \mathbf{L}^{(\tau s)} \mathbf{u}^{(s)} + \mathbf{q}^{(\tau)} = \sum_{s=0}^2 \mathbf{M}^{(\tau s)} \ddot{\mathbf{u}}^{(s)}, \text{ for } \tau = 0, 1, 2 \quad (17)$$

where  $\mathbf{L}^{(\tau s)} = \mathbf{D}_\Omega^* \mathbf{A}^{(\tau s)} \mathbf{D}_\Omega$  is the fundamental operator. It is noted that the total number of equilibrium equations depends on the expansion order  $\tau$ . For the case under consideration the static differential system (17) takes the form

$$\begin{bmatrix} \mathbf{L}^{(00)} & \mathbf{L}^{(01)} & \mathbf{L}^{(02)} \\ \mathbf{L}^{(10)} & \mathbf{L}^{(11)} & \mathbf{L}^{(12)} \\ \mathbf{L}^{(20)} & \mathbf{L}^{(21)} & \mathbf{L}^{(22)} \end{bmatrix} \begin{bmatrix} \mathbf{u}^{(0)} \\ \mathbf{u}^{(1)} \\ \mathbf{u}^{(2)} \end{bmatrix} + \begin{bmatrix} \mathbf{q}^{(0)} \\ \mathbf{q}^{(1)} \\ \mathbf{q}^{(2)} \end{bmatrix} = \begin{bmatrix} \mathbf{M}^{(00)} & \mathbf{M}^{(01)} & \mathbf{M}^{(02)} \\ \mathbf{M}^{(10)} & \mathbf{M}^{(11)} & \mathbf{M}^{(12)} \\ \mathbf{M}^{(20)} & \mathbf{M}^{(21)} & \mathbf{M}^{(22)} \end{bmatrix} \begin{bmatrix} \ddot{\mathbf{u}}^{(0)} \\ \ddot{\mathbf{u}}^{(1)} \\ \ddot{\mathbf{u}}^{(2)} \end{bmatrix} \quad (18)$$

It is worth to note that the UF by Carrera allows a simple way to obtain the differential operators related to stiffnesses and masses. It was discovered that the equations of motion follow a common pattern and that the differential operators in the collocation procedure can be obtained as a reproducing kernel (so-called fundamental nuclei). The set (18) of three fundamental nuclei allows the definition (without going through variational procedures) of any shear deformation theory, just by defining the  $F_\tau$  functions.

In order to complete the formulation, the boundary conditions need to be defined. Since the natural boundary conditions are functions of the outward unit normal vector of each plate side, two separate conditions are presented for each case:

Clamped boundary condition (C)

$$\begin{aligned} u^{(\tau)} = 0, v^{(\tau)} = 0, w^{(\tau)} = 0, \text{ at } x = 0 \text{ or } x = L_x, 0 \leq y \leq L_y \\ u^{(\tau)} = 0, v^{(\tau)} = 0, w^{(\tau)} = 0, \text{ at } y = 0 \text{ or } y = L_y, 0 \leq x \leq L_x \end{aligned} \quad (19)$$

for  $\tau = 0, 1, 2$



Soft-simply supported boundary condition (S)

$$\begin{aligned}
N_x^{(\tau)} = 0, v^{(\tau)} = 0, w^{(\tau)} = 0, \text{ at } x = 0 \text{ or } x = L_x, 0 \leq y \leq L_y \\
u^{(\tau)} = 0, N_y^{(\tau)} = 0, w^{(\tau)} = 0, \text{ at } y = 0 \text{ or } y = L_y, 0 \leq x \leq L_x \\
\text{for } \tau = 0, 1, 2
\end{aligned} \tag{20}$$

Free boundary condition (F)

$$\begin{aligned}
N_x^{(\tau)} = 0, N_{xy}^{(\tau)} = 0, T_x^{(\tau)} = 0, \text{ at } x = 0 \text{ or } x = L_x, 0 \leq y \leq L_y \\
N_{yx}^{(\tau)} = 0, N_y^{(\tau)} = 0, T_y^{(\tau)} = 0, \text{ at } y = 0 \text{ or } y = L_y, 0 \leq x \leq L_x \\
\text{for } \tau = 0, 1, 2
\end{aligned} \tag{21}$$

By using some numerical strategies as here with the GDQ method, many laminated plates can be automatically solved by expanding the nuclei and using adequate interpolations.

### 3. The generalized differential quadrature method

The generalized differential quadrature (GDQ) method has been derived by Shu [20] from the differential quadrature method presented by Bellman et al. in the 1970s [21]. This very powerful numerical technique permits to evaluate partial and total derivatives through a sum of functional values multiplied by certain weights. The interested reader can find a brief review on GDQ applications in [25–28]. The basic idea of the GDQ method is related to the integral quadrature, which is well-known in literature for the evaluation of integrals. Following the idea of the integral quadrature, the first order derivative of one-variable functions, e.g.  $f(x)$ , can be written as

$$\left. \frac{df(x)}{dx} \right|_{x=x_i} = f_x^{(1)}(x_i) = \sum_{j=1}^N a_{ij}^{x,(1)} f(x_j) \quad \text{for } i = 1, 2, \dots, N \tag{22}$$

where  $a_{ij}^{x,(1)}$  represent the weighting coefficients,  $N$  is the total number of grid points  $x_1, x_2, \dots, x_N$  in the whole domain and  $f(x_j)$  is the calculated value of  $f(x)$  at the point  $x = x_j$ . From equation (22) it appears that, when the weighting coefficients are computed, the derivative of the  $f(x)$  function at the point  $x = x_i$  is given by the sum of values calculated

according to the right-hand expression (22). Thus, it is compulsory to have a well-defined grid point distribution all over the given domain. Some GDQ grid distributions are reported in [29–32, 37, 38]. To compute the first order weighting coefficients  $a_{ij}^{x,(1)}$ , the following algebraic formulae [20] are derived

$$\begin{aligned} a_{ij}^{x,(1)} &= \frac{L^{(1)}(x_i)}{(x_i - x_j)L^{(1)}(x_j)} & \text{for } i, j = 1, 2, \dots, N \text{ and } i \neq j \\ a_{ii}^{x,(1)} &= - \sum_{k=1, k \neq i}^N a_{ik}^{(1)} & \text{for } i = j \end{aligned} \quad (23)$$

where the Lagrange interpolation polynomials were used as test functions

$$L^{(1)}(x_i) = \prod_{q=1, q \neq i}^N (x_q - x_i), \quad L^{(1)}(x_j) = \prod_{q=1, q \neq j}^N (x_q - x_j) \quad (24)$$

The weighting coefficients of the second and higher order derivatives can be computed from a recurrence relationship [20]. A generalized higher order derivative can be written as

$$\begin{aligned} \left. \frac{d^n f(x)}{dx^n} \right|_{x=x_i} &= f_x^{(n)}(x_i) = \sum_{j=1}^N a_{ij}^{x,(n)} f(x_j) \\ &\text{for } i = 1, 2, \dots, N, \quad n = 2, 3, \dots, N-1 \end{aligned} \quad (25)$$

The general approach by Shu [20], which is based on the polynomial approximation, allows to write the following weighting coefficients

$$\begin{aligned} a_{ij}^{x,(n)} &= n \left( a_{ii}^{x,(n-1)} a_{ij}^{x,(1)} - \frac{a_{ij}^{x,(n-1)}}{x_i - x_j} \right) & \text{for } i \neq j, \quad n = 2, 3, \dots, N-1 \\ a_{ii}^{x,(n)} &= - \sum_{k=1, k \neq i}^N a_{ik}^{x,(n)} & \text{for } i = j \end{aligned} \quad (26)$$

As shown by Shu [20], the one-dimensional problem can be directly extended to the multi-dimensional case for a regular shape, such as a rectangle or a circle. In general, a function  $f(x, y)$  can be defined on the given domain and its values depend on the points along  $x$  and  $y$ . In the following,  $N$  points along  $x$  direction and  $M$  points along  $y$  direction are assumed. It is noted that the derivatives of any order along  $x$  and  $y$  can be written using Shu's notation

[20]

$$\begin{aligned}
f_x^{(n)}(x_i, y_j) &= \left. \frac{\partial^{(n)} f(x, y)}{\partial x^n} \right|_{\substack{x=x_i \\ y=y_j}} = \sum_{k=1}^N a_{ik}^{x,(n)} f(x_k, y_j) \\
&\text{for } i = 1, 2, \dots, N \quad n = 1, 2, \dots, N-1 \\
f_y^{(m)}(x_i, y_j) &= \left. \frac{\partial^{(m)} f(x, y)}{\partial y^m} \right|_{\substack{x=x_i \\ y=y_j}} = \sum_{l=1}^M a_{jl}^{y,(m)} f(x_i, y_l) \\
&\text{for } j = 1, 2, \dots, M \quad m = 1, 2, \dots, M-1
\end{aligned} \tag{27}$$

where  $a_{ik}^{x,(n)}$  and  $a_{jl}^{y,(m)}$  are the weighting coefficients of order  $n$  and  $m$  along  $x$  and  $y$ , respectively. Furthermore, following the same rule in equation (27), the mixed derivative can be written as follows

$$\begin{aligned}
f_{xy}^{(n+m)}(x_i, y_j) &= \left. \frac{\partial^{(n+m)} f(x, y)}{\partial x^n \partial y^m} \right|_{\substack{x=x_i \\ y=y_j}} = \sum_{k=1}^N a_{ik}^{x,(n)} \left( \sum_{l=1}^M a_{jl}^{y,(m)} f(x_k, y_l) \right) \\
&\text{for } i = 1, 2, \dots, N \quad j = 1, 2, \dots, M \\
&\text{for } n = 1, 2, \dots, N-1 \quad m = 1, 2, \dots, M-1
\end{aligned} \tag{28}$$

where  $a_{ik}^{x,(n)}$  and  $a_{jl}^{y,(m)}$  have the same meaning in expressions (27).

### 3.1. Grid distributions

The numerical accuracy of the GDQ method is usually sensitive to the grid point distribution choice in the given domain. However, it has been proven in [29–32] that the Chebyshev-Gauss-Lobatto (C-G-L) grid point distribution gives accurate results in most of cases. In general, the natural and simplest choice of uniform grids does not lead to stable and accurate results for any GDQ computation. In the numerical results proposed in this paper a C-G-L grid distribution is considered for both directions  $x$  and  $y$

$$\begin{aligned}
x_i &= \frac{1}{2} \left( 1 - \cos \left( \frac{i-1}{N-1} \pi \right) \right) \\
y_j &= \frac{1}{2} \left( 1 - \cos \left( \frac{j-1}{M-1} \pi \right) \right)
\end{aligned} \tag{29}$$

where  $N, M$  are the total number of points in the given directions  $x, y$ , respectively.

### 3.2. The static problem

In this paper the GDQ formulation is used to compute elliptic boundary-value problems. Considering a linear elliptic partial differential operator  $\ell$ , that contains all the spatial derivatives of the problem, a given function  $q(\mathbf{x})$  and the configuration variable or variables  $u(\mathbf{x})$ , the differential problem within its boundary conditions can be written as

$$\begin{cases} \ell(u(\mathbf{x})) + q(\mathbf{x}) = 0 & \text{in } \Omega \\ \ell_B(u(\mathbf{x})) = \mathbf{g} & \text{on } \partial\Omega \end{cases} \quad (30)$$

In static problems we seek the computation of displacements  $u$  from the global system of equations, where  $\ell$ ,  $\ell_B$  are linear operators in the domain and on the boundary, respectively. In equations (30),  $q(\mathbf{x})$  and  $\mathbf{g}$  usually represent the external forces applied on the mechanical system and the boundary conditions, respectively. The boundary-value problem (30), is replaced by an algebraic system of equations. The GDQ method is used to discretize the spatial derivatives in the differential operator  $\ell$  at the interior grid points of the discrete domain. The following set of algebraic equations is obtained

$$\begin{cases} \mathcal{L}\mathbf{U} + \mathbf{Q} = \mathbf{0} \\ \mathcal{L}_B\mathbf{U} = \mathbf{G} \end{cases} \quad (31)$$

where  $\mathbf{U}$  is a vector representing a set of unknown functional values at all the interior points,  $\mathcal{L}$  is a matrix resulting from the DQ discretization of the elliptic operator and  $\mathbf{Q}, \mathbf{G}$  are the known vectors arising from the functions  $q(\mathbf{x})$  and  $\mathbf{g}$ , respectively. The algebraic systems (31) are written using the stiffness matrix notation

$$\mathbf{K}\mathbf{U} = \bar{\mathbf{Q}} \quad (32)$$

The equation (32) can be directly solved by Gauss elimination technique. For further details of static problem resolutions about plates and shells, it can be seen the paper by Viola et al. [38].

### 3.3. The eigenproblem

The eigenvalue problem can be achieved from the equation of motion of a given system in which the external forces are set to zero

$$\ell(u(\mathbf{x}, t)) = \rho \ddot{u}(\mathbf{x}, t) \quad (33)$$

where the right-hand term represents the inertia term. The eigenproblem looks for eigenvalues ( $\lambda$ ) and eigenvectors  $U(\mathbf{x})$  and it is based on the following assumption

$$u(\mathbf{x}, t) = U(\mathbf{x})e^{i\lambda t} \quad (34)$$

Substituting the relation (34) into the equation (33) a generalized eigenvalue problem can be achieved with the corresponding boundary conditions

$$\begin{cases} \ell(U(\mathbf{x})) + \rho\lambda^2 U(\mathbf{x}) = 0 & \text{in } \Omega \\ \ell_B U(\mathbf{x}) = 0 & \text{on } \partial\Omega \end{cases} \quad (35)$$

As in the static problem, the eigenproblem defined in (35) is replaced by a finite-dimensional eigenvalue problem, based on the GDQ approximation as follows

$$\begin{cases} \mathcal{L}\mathbf{U} + \lambda^2 \mathbf{M}\mathbf{U} = \mathbf{0} \\ \mathcal{L}_B \mathbf{U} = 0 \end{cases} \quad (36)$$

where  $\mathbf{M}$  represents the mass matrix of the physical system under study. In conclusion, solving the above presented generalized eigenvalue problem the eigenvalues and eigenvectors of the given system can be obtained. Finally, the reader can refer to [37] for solutions of eigenvalue problems regarding plates and shells.

## 4. Numerical examples

### 4.1. Static problems of isotropic plates

The first example considers the deflections of simply-supported and clamped, uniformly loaded square plates ( $a/b = 1$ ,  $\nu = 0.3$ ). Thin ( $h/a = 0.01$ ) and thick ( $h/a = 0.5$ ) plates are considered, using  $7 \times 7$ ,  $11 \times 11$ ,  $15 \times 15$  and  $19 \times 19$  points. Tables 1 and 2 compare the

present results with the Mindlin (FSDT) theory [46] and the analytical higher-order (HSDT) solution by Kant et al. [6, 7]. The deflections are presented in their dimensionless form  $\bar{w} = w_{\max}D/qa^4$ , where  $D$  is the flexural stiffness ( $D = Eh^3/(12(1 - \nu^2))$ ),  $q$  is the vertical load and  $a$  is the side of the square plate. The results show that the present HSDT solution has good convergence characteristics. Moreover, the present HSDT numerical technique reproduces almost exactly the analytical solution by Kant.

#### 4.2. Free vibration problems of isotropic plates

Natural frequencies and vibration modes are presented for isotropic square simply-supported and clamped plates ( $a/b = 1$ ). The non-dimensional frequency parameters are given as

$$\bar{\omega} = \omega a \sqrt{\rho/G} \quad (37)$$

where  $\omega$  is the circular frequency ( $\omega = 2\pi f$ ,  $f$  is the frequency),  $a$  is still the side length,  $\rho$  is the mass density per unit of volume,  $G$  is the shear modulus and  $G = E/(2(1 + \nu))$ ,  $E$  being the Young's modulus and  $\nu$  the Poisson's ratio. The results for isotropic plates with various boundary conditions are computed. Firstly, two fully clamped (CCCC) Mindlin/Reissner square plates with different thickness-to-side ratios are considered. The plates are clamped at all boundary edges. The first four modes of vibration for both plates are calculated. Two cases of thickness-to-side ratios  $h/a = 0.01$  and  $0.1$  are examined. The comparison of frequency parameters with the Rayleigh-Ritz solutions [47] and results by Liew et al. [48], using a reproducing kernel particle approximation, for each plate is listed in table 3. Excellent agreement is obtained even if a small number of nodes is used. The current solution is closer to Rayleigh-Ritz solutions than that of Liew. Secondly, fully simply supported (SSSS) Mindlin/Reissner square plates with different thickness-to-side ratios are considered. The first four modes of vibration are computed for two cases of thickness-to-side ratios  $h/a = 0.01$  and  $0.1$ . Results are compared with 3D-elasticity and Mindlin closed form solutions [49], and results by Liew et al. [48]. The results listed in table 4 show excellent agreement with closed form solutions.

#### 4.3. Static problems of cross-ply laminated plates

A simply supported square laminated plate of side  $a$  and thickness  $h$  is composed of four equally layers oriented at  $(0/90/90/0)$ . The plate is subjected to a sinusoidal vertical pressure of the form

$$q = P \sin\left(\frac{\pi x}{a}\right) \sin\left(\frac{\pi y}{a}\right)$$

with the origin of the coordinate system located at the lower left corner on the midplane and  $P$  the maximum load (at center of plate). The orthotropic material properties are given by

$$E_1 = 25.0E_2 \quad G_{12} = G_{13} = 0.5E_2 \quad G_{23} = 0.2E_2 \quad \nu_{12} = 0.25$$

The in-plane displacements, the transverse displacements, the normal stresses and the in-plane and transverse shear stresses are presented in normalized form as

$$\begin{aligned} \bar{w} &= \frac{10^2 w_{(a/2, a/2, 0)} h^3 E_2}{Pa^4}, \quad \bar{\sigma}_{xx} = \frac{\sigma_{xx(a/2, a/2, h/2)} h^2}{Pa^2}, \quad \bar{\sigma}_{yy} = \frac{\sigma_{yy(a/2, a/2, h/4)} h^2}{Pa^2} \\ \bar{\tau}_{xz} &= \frac{\tau_{xz(0, a/2, 0)} h}{Pa}, \quad \bar{\tau}_{xy} = \frac{\tau_{xy(0, 0, h/2)} h^2}{Pa^2} \end{aligned} \quad (38)$$

In table 5 the present HSDT results, using  $7 \times 7$  up to  $19 \times 19$  points, are compared with higher-order solutions by Ahkras [50], and Reddy [51], FSDT solutions by Reddy and Chao [52] and an exact solution by Pagano [53]. Furthermore, the results obtained according to Radial basis function (RBFs) collocation with Reddy's theory [22], and a layerwise theory [23] are also put in the comparison. As expected, the present HSDT displacements are very good for thin or thick plates. Highly accurate normal stresses and transverse shear stresses are obtained.

#### 4.4. Free vibration problems of cross-ply laminated plates

Unless otherwise stated, all layers of the laminate are assumed to be of the same thickness, density and made of the same linearly elastic composite material. The following material parameters of a layer are used:

$$\frac{E_1}{E_2} = 10, 20, 30 \text{ or } 40; G_{12} = G_{13} = 0.6E_2; G_{23} = 0.5E_2; \nu_{12} = 0.25 \quad (39)$$

The subscripts 1 and 2 denote the normal and transverse directions to the fiber direction in a lamina, which may be oriented at an angle to the plate axes. The ply angle of each layer is measured from the global  $x$ -axis to the fiber direction. The example considered is a simply supported square plate of the cross-ply lamination (0/90/90/0). The thickness and length of the plate are always denoted by  $h$  and  $a$ , respectively. The thickness-to-span ratio  $h/a = 0.2$  is adopted in the computation. Table 6 lists the fundamental frequency of the simply supported laminate made of various modulus ratios  $E_1/E_2$ . It is found that the results are in very close agreement with the values reported in [13, 54] and the meshfree results by Liew [55] based on the FSDT. Furthermore, in order to show that the given problem can be studied with mixed boundary conditions, also some mode shapes and boundary conditions are reported. The plate is square with  $a = b = 1$  m and the total plate thickness is  $h = 0.1$  m. Three different lamination schemes are taken into account and described by the notations (0/90/90/0), (0/0/90/90) and (0/90/0/90). They are made of Graphite-Epoxy with all the same thickness  $h_k = h/4$ . The orthotropic material has the following mechanical properties

$$\begin{aligned} E_1 &= 137.9 \text{ GPa}, E_2 = E_3 = 8.96 \text{ GPa}, G_{12} = G_{13} = 7.1 \text{ GPa}, G_{23} = 6.21 \text{ GPa} \\ \nu_{12} &= \nu_{13} = 0.3, \nu_{23} = 0.49, \rho = 1450 \text{ kg/m}^3 \end{aligned} \quad (40)$$

Moreover, three different boundary conditions (BCs) are enforced. The first BC is a CFFF (clamped on one edge and free on the other three edges) for the (0/90/90/0) laminate. The second BC is a CFFC (clamped on two adjacent edges and free on the other two) for the (0/0/90/90) laminate. The third BC is a CFCC (clamped on three edges and free on a single edge) for the (0/90/0/90) laminate. The GDQ numerical results are obtained using a  $31 \times 31$  Chebyshev-Gauss-Lobatto grid distribution [25–32, 37–39]. The results are compared with a 3D Finite Element Solution (FEM) obtained with a mesh of 59,049 nodes with three degrees of freedom per node. The first six mode shapes, for each case, are depicted in figures 2-4 in which the correspondent frequency is reported below each modal shape within the reference FEM numerical solution. Very good agreement is observed for all the computations. It is worth emphasizing that a two-dimensional higher-order solution is compared to a three



dimensional one.

## 5. Conclusions

In this paper, the generalized differential quadrature method is used to analyse static deformations and free vibrations of thick plates. A higher-order shear and normal deformation theory, allowing for transverse normal deformations is presented. Square isotropic and cross-ply laminated plates in bending and free vibrations are analyzed. The present results were compared with existing analytical solutions or competitive finite element solutions and very good agreement was observed in both cases.

## References

- [1] E. Carrera and B. Kroplin. Zig-zag and interlaminar equilibria effects in large deflection and post-buckling analysis of multilayered plates. *Mechanics of Composite Materials and Structures*, 4:69–94, 1997.
- [2] E. Carrera. Evaluation of layer-wise mixed theories for laminated plate analysis. *AIAA Journal*, (36):830–839, 1998.
- [3] E. Carrera. Developments, ideas, and evaluations based upon Reissner’s mixed variational theorem in the modelling of multilayered plates and shells. *Applied Mechanics Reviews*, 54:301–329, 2001.
- [4] E. Carrera. Historical review of zig-zag theories for multilayered plates and shells. *Applied Mechanics Reviews*, 56:287–308, 2003.
- [5] F.A. Fazzolari, E. Carrera. Free vibration analysis of sandwich plates with anisotropic face sheets in thermal environment by using the hierarchical trigonometric Ritz formulation. *Composites Part B Engineering*, 50:67–81, 2013.
- [6] T. Kant. Numerical analysis of thick plates. *Computer Methods in Applied Mechanics and Engineering*, 31:1–18, 1982.
- [7] T. Kant, D. R. J. Owen and O. C. Zienkiewicz. A refined higher-order  $C^0$  plate element. *Computers and Structures*, 15(2):177–183, 1982.
- [8] K. H. Lo, R. M. Christensen and E. M. Wu. A high-order theory of plate deformation, part I: Homogeneous plates. *Journal of Applied Mechanics*, 44(7):663–668, 1977.
- [9] K. H. Lo, R. M. Christensen and E. M. Wu. A high-order theory of plate deformation, part II: Laminated plates. *Journal of Applied Mechanics*, 44(4):669–676, 1977.

- [10] R. C. Batra and S. Vidoli. Higher order piezoelectric plate theory derived from a three-dimensional variational principle. *AIAA Journal*, 40:91–104, 2002.
- [11] E. Carrera.  $C^0$  Reissner-Mindlin multilayered plate elements including zig-zag and interlaminar stress continuity. *International Journal of Numerical Methods in Engineering*, 39:1797–1820, 1996.
- [12] L. Librescu, A. A. Khdeir and J. N. Reddy. A comprehensive analysis of the state of stress of elastic anisotropic flat plates using refined theories. *Acta Mechanica*, 70:57–81, 1987.
- [13] J. N. Reddy. *Mechanics of Laminated Composite Plates: Theory and Analysis*. CRC Press, Boca Raton, 1997.
- [14] L. Fiedler, W. Lacarbonara and F. Vestroni. A generalized higher-order theory for multi-layered, shear-deformable composite plates. *Acta Mechanica*, 209:85–98, 2010.
- [15] E. Carrera, S. Brischetto, M. Cinefra, M. Soave. Effects of thickness stretching in functionally graded plates and shells. *Composites Part B Engineering*, 42:123–133, 2011.
- [16] G. Giunta, F. Biscani, S. Belouettar, E. Carrera. Hierarchical modelling of doubly curved laminated composite shells under distributed and localised loadings. *Composites Part B Engineering*, 42:682–691, 2011.
- [17] G. Giunta, F. Biscani, S. Belouettar, A.J.M. Ferreira, E. Carrera. Free vibration analysis of composite beams via refined theories. *Composites Part B Engineering*, 44:540–552, 2013.
- [18] D.A. Maturi, A.J.M. Ferreira, A.M. Zenkour, D.S. Mashat. Analysis of sandwich plates with a new layerwise formulation. *Composites Part B Engineering*, In Press, 2013.
- [19] L.V. Tran, A.J.M. Ferreira, H. Nguyen-Xuan. Isogeometric analysis of functionally graded plates using higher-order shear deformation theory. *Composites Part B Engineering*, 51:368–383, 2013.
- [20] C. Shu. *Differential quadrature and its application in engineering*. Springer, 2000.
- [21] R. E. Bellman, B. G. Kashef and J. Casti, Differential quadrature: A technique for the rapid solution of nonlinear partial differential equations. *Journal of Computational Physics*, 10:40–52, 1972.
- [22] A. J. M. Ferreira, C. M. C. Roque and P. A. L. S. Martins. Analysis of composite plates using higher-order shear deformation theory and a finite point formulation based on the multiquadric radial basis function method. *Composites: Part B*, 34:627–636, 2003.
- [23] A. J. M. Ferreira. Analysis of composite plates using a layerwise deformation theory and multiquadrics discretization. *Mechanics of Advanced Materials and Structures*, 12(2):99–112, 2005.

- [24] C.M.C. Roque, A.J.M. Ferreira, R.M.N. Jorge. Modelling of composite and sandwich plates by a trigonometric layerwise deformation theory and radial basis functions. *Composites Part B Engineering*, 36:559–572, 2005.
- [25] F. Tornabene. *Meccanica delle Strutture a Guscio in Materiale Composito. Il Metodo Generalizzato di Quadratura Differenziale*, Esculapio, Bologna, 2012.
- [26] F. Tornabene. Vibration analysis of functionally graded conical, cylindrical and annular shell structures with a four-parameter power-law distribution. *Computer Methods in Applied Mechanics and Engineering* 198:2911–2935, 2009.
- [27] E. Viola and F. Tornabene. Vibration analysis of damaged circular arches with varying cross-section. *Structural Integrity & Durability (SID-SDHM)*, 1:155–169, 2005.
- [28] E. Viola and F. Tornabene. Vibration analysis of conical shell structures using GDQ method. *Far East Journal of Applied Mathematics*, 25:23–39, 2006.
- [29] F. Tornabene and E. Viola. Vibration analysis of spherical structural elements using the GDQ method. *Computers & Mathematics with Applications*, 53:1538–1560, 2007.
- [30] E. Viola, M. Dilella and F. Tornabene. Analytical and numerical results for vibration analysis of multi-stepped and multi-damaged circular arches. *Journal of Sound and Vibration*, 299:143–163, 2007.
- [31] F. Tornabene and E. Viola. 2-D solution for free vibrations of parabolic shells using generalized differential quadrature method. *European Journal of Mechanics - A/Solids*, 27:1001–102, 2008.
- [32] F. Tornabene. 2-D GDQ solution for free vibrations of anisotropic doubly-curved shells and panels of revolution. *Composite Structures*, 93:1854–1876, 2011.
- [33] A.J.M. Ferreira, E. Carrera, M. Cinefra, C.M.C. Roque, O. Polit. Analysis of laminated shells by a sinusoidal shear deformation theory and radial basis functions collocation, accounting for through-the-thickness deformations. *Composites Part B Engineering*, 42:1276–1284, 2011.
- [34] A.J.M. Ferreira, C.M.C. Roque, A.M.A. Neves, R.M.N. Jorge, C.M.M. Soares, K.M. Liew. Buckling and vibration analysis of isotropic and laminated plates by radial basis functions. *Composites Part B Engineering*, 42:592–606, 2011.
- [35] F. Tornabene, A. Liverani, G. Caligiana. Laminated Composite Rectangular and Annular Plates: A GDQ Solution for Static Analysis with a Posteriori Shear and Normal Stress Recovery. *Composites Part B Engineering* 43:1847–1872, 2012.
- [36] A.M.A. Neves, A.J.M. Ferreira, E. Carrera, C.M.C. Roque, M. Cinefra, R.M.N. Jorge, C.M.M. Soares. A quasi-3D sinusoidal shear deformation theory for the static and free vibration analysis of functionally graded plates. *Composites Part B Engineering*, 43:711–725, 2012.

- [37] E. Viola, F. Tornabene and N. Fantuzzi. General higher-order shear deformation theories for the free vibration analysis of completely doubly-curved laminated shells and panels. *Composite Structures*, 95:639–666, 2013.
- [38] E. Viola, F. Tornabene and N. Fantuzzi. Static analysis of completely doubly-curved laminated shells and panels using general higher-order shear deformation theories. *Composite Structures*, 101:59–93, 2013.
- [39] F. Tornabene, E. Viola and N. Fantuzzi. General higher-order equivalent single layer theory for free vibrations of doubly-curved laminated composite shells and panels. *Composite Structures*, 104:94–117, 2013.
- [40] E. Viola, F. Tornabene, N. Fantuzzi. Generalized Differential Quadrature Finite Element Method for Cracked Composite Structures of Arbitrary Shape. *Composite Structures* 106:815–834, 2013.
- [41] F. Tornabene, N. Fantuzzi, E. Viola, A.J.M. Ferreira. Radial Basis Function Method Applied to Doubly-Curved Laminated Composite Shells and Panels with a General Higher-Order Equivalent Single Layer Theory. *Composites Part B Engineering* 55:642–659, 2013.
- [42] F. Tornabene, N. Fantuzzi, E. Viola, J.N. Reddy. Winkler-Pasternak Foundation Effect on the Static and Dynamic Analyses of Laminated Doubly-Curved and Degenerate Shells and Panels. *Composites Part B Engineering*, <http://dx.doi.org/10.1016/j.compositesb.2013.06.020>, In Press, 2013.
- [43] A.J.M. Ferreira, E. Viola, F. Tornabene, N. Fantuzzi, A.M. Zenkour. Analysis of Sandwich Plates by Generalized Differential Quadrature Method *Mathematical Problems in Engineering* 2013:1-22,[Article ID 964367], <http://dx.doi.org/10.1155/2013/964367>.
- [44] F. Tornabene, N. Fantuzzi, E. Viola, E. Carrera. Static Analysis of Doubly-Curved Anisotropic Shells and Panels Using CUF Approach, Differential Geometry and Differential Quadrature Method. *Composite Structures*, 107:675–697, 2014.
- [45] A.M.A. Neves, A.J.M. Ferreira, E. Carrera, M. Cinefra, C.M.C. Roque, R.M.N. Jorge, C.M.M. Soare. Static, free vibration and buckling analysis of isotropic and sandwich functionally graded plates using a quasi-3D higher-order shear deformation theory and a meshless technique. *Composites Part B Engineering*, 44:657–674, 2013.
- [46] R. D. Mindlin. Influence of rotary inertia and shear in flexural motions of isotropic elastic plates. *Journal of Applied mechanics*, 18:31–38, 1951.
- [47] D. J. Dawe and O. L. Roufaeil. Rayleigh-ritz vibration analysis of mindlin plates. *Journal of Sound and Vibration*, 69(3):345–359, 1980.
- [48] K. M. Liew, J. Wang, T. Y. Ng and M. J. Tan. Free vibration and buckling analyses of shear-deformable plates based on FSDT meshfree method. *Journal of Sound and Vibration*, 276:997–1017, 2004.

- [49] E. Hinton. *Numerical methods and software for dynamic analysis of plates and shells*. Pineridge Press, 1988.
- [50] G. Akhras, M. S. Cheung and W. Li. Finite strip analysis for anisotropic laminated composite plates using higher-order deformation theory. *Computers & Structures*, 52(3):471–477, 1994.
- [51] J. N. Reddy. A simple higher-order theory for laminated composite plates. *Journal of Applied Mechanics*, 51:745–752, 1984.
- [52] J. N. Reddy and W. C. Chao. A comparison of closed-form and finite-element solutions of thick laminated anisotropic rectangular plates. *Nuclear Engineering and Design*, 64:153–167, 1981.
- [53] N. J. Pagano. Exact solutions for rectangular bidirectional composites and sandwich plates. *Journal of Composite Materials*, 4:20–34, 1970.
- [54] A. A. Khdeir and L. Librescu. Analysis of symmetric cross-ply elastic plates using a higher-order theory, part II: buckling and free vibration. *Composite Structures*, 9:259–277, 1988.
- [55] K. M. Liew, Y. Q. Huang and J. N. Reddy. Vibration analysis of symmetrically laminated plates based on FSDT using the moving least squares differential quadrature method. *Computer Methods in Applied Mechanics and Engineering*, 192:2203–2222, 2003.

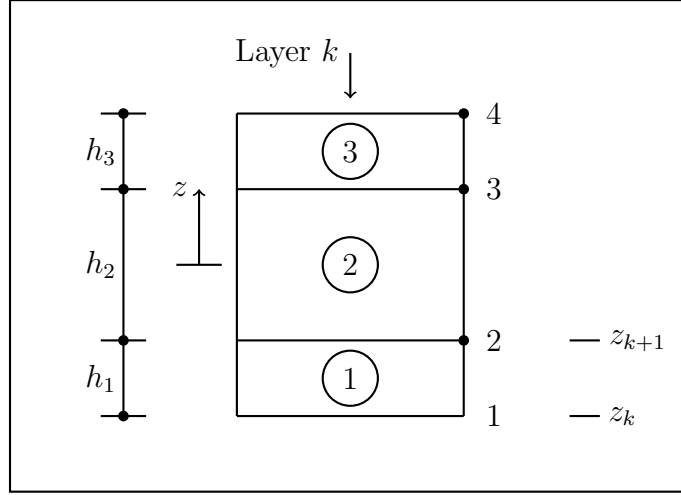


Figure 1: A 3-layer laminate.

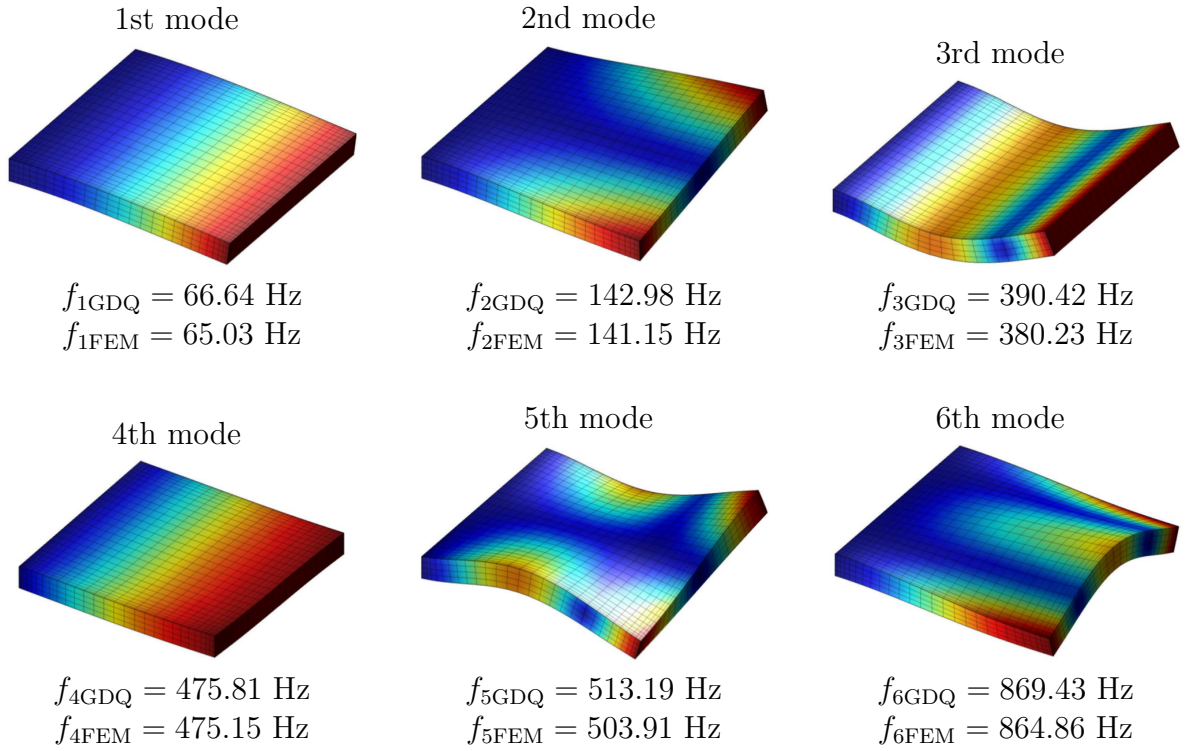


Figure 2: First six mode shapes of a CFFF square plate with (0/90/90/0) lamination scheme.

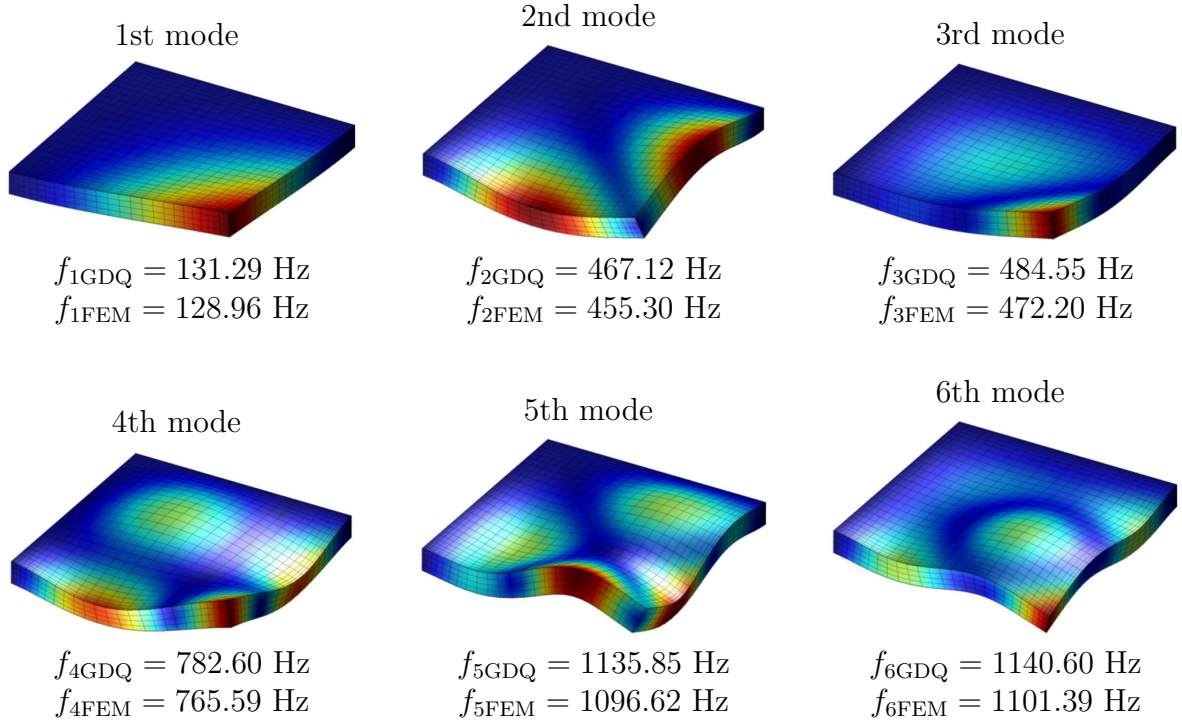


Figure 3: First six mode shapes of a CFFC square plate with (0/0/90/90) lamination scheme.

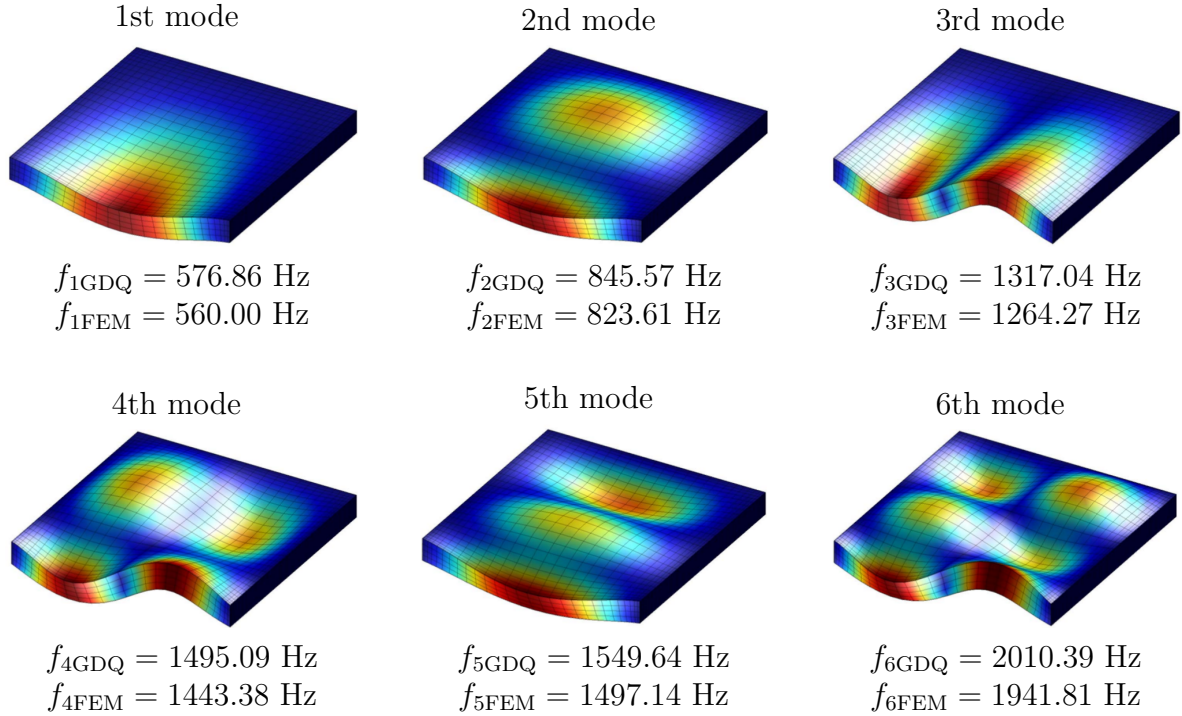


Figure 4: First six mode shapes of a CFCC square plate with (0/90/0/90) lamination scheme.

$h/a$	Source	$7 \times 7$	$11 \times 11$	$15 \times 15$	$19 \times 19$
0.01	Present HSDT	0.004058	0.004064	0.004064	0.004064
	Mindlin [46]	0.00406			
0.1	Present HSDT	0.004248	0.004251	0.004249	0.004249
	Mindlin [46]	0.00427			
0.2	Present HSDT	0.004816	0.004810	0.004805	0.004804
	Mindlin [46]	0.00490			
0.5	Present HSDT	0.00859	0.008528	0.008522	0.008522
	Kant [6, 7]	0.00853			

Table 1: Convergence study for deflections ( $\times qa^4/D$ ) for uniformly loaded square SSSS plate ( $\nu = 0.3$ ). The classical plate solution is 0.00406. Note that the load is applied at  $z = h/2$  surface (top surface).

$h/a$	Source	$7 \times 7$	$11 \times 11$	$15 \times 15$	$19 \times 19$
0.01	Present HSDT	0.001254	0.001262	0.001264	0.001265
	Mindlin [46]	0.00126			
0.1	Present HSDT (at $z = h/2$ )	0.001483	0.001488	0.001488	0.001506
	Kant [6, 7]	0.00156			
0.2	Present HSDT (at $z = h/2$ )	0.002118	0.002120	0.002119	0.002119
	Kant [6, 7]	0.00211			
0.5	Present HSDT(at $z = h/2$ )	0.006107	0.006090	0.006089	0.006089
	Kant [6, 7]	0.00609			

Table 2: Convergence study for deflections ( $\times qa^4/D$ ) for uniformly loaded square CCCC plate ( $\nu = 0.3$ ). The classical plate solution is 0.00126.

Mode no.	$7 \times 7$	$11 \times 11$	$15 \times 15$	Rayleigh-Ritz [47]	Liew et al. [48]
Present HSDT ( $a/h = 10$ )					
1	1.6065	1.5952	1.5944	1.5940	1.5582
2	3.1450	3.0380	3.0373	3.0390	3.0182
3	3.1450	3.0380	3.0373	3.0390	3.0182
4	4.3594	4.2519	4.2515	4.2650	4.1711
Present HSDT ( $a/h = 100$ )					
1	0.1779	0.1762	0.1758	0.1754	0.1743
2	0.3898	0.3592	0.3582	0.3576	0.3576
3	0.3898	0.3592	0.3582	0.3576	0.3576
4	0.5589	0.5293	0.5277	0.5274	0.5240

Table 3: Natural frequencies of a CCCC square Mindlin/Reissner plate with  $\nu = 0.3$ .



Mode no.	$7 \times 7$	$11 \times 11$	$15 \times 15$	3D [53]	Mindlin [49]	Liew et al. [48]
Present HSDT ( $a/h = 10$ )						
1	0.9286	0.9286	0.9286	0.932	0.930	0.922
2	2.1990	2.2111	2.2111	2.226	2.219	2.205
3	2.1990	2.2111	2.2111	2.226	2.219	2.205
4	3.3745	3.3885	3.3885	3.421	3.406	3.377
Present HSDT ( $a/h = 100$ )						
1	0.0963	0.0963	0.0963		0.0963	0.0961
2	0.2381	0.2406	0.2406		0.2406	0.2419
3	0.2381	0.2406	0.2406		0.2406	0.2419
4	0.3811	0.3847	0.3847		0.3848	0.3860

Table 4: Natural frequencies of a SSSS square Mindlin/Reissner plate with  $\nu = 0.3$ .

$\frac{a}{h}$	Method	$\bar{w}$	$\bar{\sigma}_{xx}$	$\bar{\sigma}_{yy}$	$\bar{\tau}_{zx}$	$\bar{\tau}_{xy}$
4	HSDT Finite Strip method [50]	1.8939	0.6806	0.6463	0.2109	0.0450
	HSDT [51]	1.8937	0.6651	0.6322	0.2064	0.0440
	FSDT [52]	1.7100	0.4059	0.5765	0.1398	0.0308
	elasticity [53]	1.954	0.720	0.666	0.270	0.0467
	Ferreira et al. [22] ( $N = 21$ )	1.8864	0.6659	0.6313	0.1352	0.0433
	Ferreira (layerwise) [23] ( $N = 21$ )	1.9075	0.6432	0.6228	0.2166	0.0441
	present ( $7 \times 7$ grid)	1.8865	0.7142	0.6322	0.2142	0.0462
	present ( $11 \times 11$ grid)	1.8869	0.7148	0.6328	0.2142	0.0462
	present ( $15 \times 15$ grid)	1.8869	0.7148	0.6328	0.2142	0.0462
	present ( $19 \times 19$ grid)	1.8869	0.7148	0.6328	0.2142	0.0462
10	HSDT Finite Strip method [50]	0.7149	0.5589	0.3974	0.2697	0.0273
	HSDT [51]	0.7147	0.5456	0.3888	0.2640	0.0268
	FSDT [52]	0.6628	0.4989	0.3615	0.1667	0.0241
	elasticity [53]	0.743	0.559	0.403	0.301	0.0276
	Ferreira et al. [22] ( $N = 21$ )	0.7153	0.5466	0.4383	0.3347	0.0267
	Ferreira (layerwise) [23] ( $N = 21$ )	0.7309	0.5496	0.3956	0.2888	0.0273
	present ( $7 \times 7$ grid)	0.7188	0.5606	0.3911	0.2843	0.0272
	present ( $11 \times 11$ grid)	0.7191	0.5612	0.3915	0.2843	0.0273
	present ( $15 \times 15$ grid)	0.7191	0.5612	0.3915	0.2843	0.0273
	present ( $19 \times 19$ grid)	0.7191	0.5612	0.3915	0.2843	0.0273
100	HSDT Finite Strip method [50]	0.4343	0.5507	0.2769	0.2948	0.0217
	HSDT [51]	0.4343	0.5387	0.2708	0.2897	0.0213
	FSDT [52]	0.4337	0.5382	0.2705	0.1780	0.0213
	elasticity [53]	0.4347	0.539	0.271	0.339	0.0214
	Ferreira et al. [22] ( $N = 21$ )	0.4365	0.5413	0.3359	0.4106	0.0215
	Ferreira (layerwise) [23] ( $N = 21$ )	0.4374	0.5420	0.2697	0.3232	0.0216
	present ( $7 \times 7$ grid)	0.4347	0.5390	0.2709	0.3154	0.0214
	present ( $11 \times 11$ grid)	0.4350	0.5396	0.2713	0.3155	0.0214
	present ( $15 \times 15$ grid)	0.4350	0.5396	0.2713	0.3155	0.0214
	present ( $19 \times 19$ grid)	0.4350	0.5396	0.2713	0.3155	0.0214

Table 5: (0/90/90/0) square laminated plate under sinusoidal load and with HSDT formulations.

Method	Grid	$E_1/E_2$			
		10	20	30	40
Liew [55]		8.2924	9.5613	10.320	10.849
Exact (Reddy, Khdeir)[13, 54]		8.2982	9.5671	10.326	10.854
Present HSDT ( $\nu_{23} = 0.18$ )	$7 \times 7$	8.3166	9.5459	10.2705	10.7663
	$11 \times 11$	8.3150	9.5443	10.2689	10.7648
	$15 \times 15$	8.3150	9.5443	10.2689	10.7648
	$19 \times 19$	8.3150	9.5443	10.2689	10.7648

Table 6: The normalized fundamental frequency of the simply-supported cross-ply laminated square plate (0/90/90/0) ( $\bar{\omega} = (\omega a^2/h)\sqrt{\rho/E_2}$ ,  $h/a = 0.2$ ).